International Journal of Heat and Mass Transfer 67 (2013) 46–60

Contents lists available at ScienceDirect

International Journal of Heat and Mass Transfer

journal homepage: www.elsevier.com/locate/ijhmt

Analysis of heat transport on local thermal non-equilibrium in porous liver during microwave ablation

Pornthip Keangin [a], Phadungsak Rattanadecho [b,*]

[a] Department of Mechanical Engineering, Faculty of Engineering, Mahidol University, 25/25 Phutthamomthon 4 Rd., Salaya, Nakhon Pathom 73170, Thailand
[b] Department of Mechanical Engineering, Faculty of Engineering, Thammasat University (Rangsit Campus), 99 moo 18, Khlong Luang, Pathum Thani 12120, Thailand

ARTICLE INFO

Article history:
Received 24 January 2013
Received in revised form 12 July 2013
Accepted 19 July 2013
Available online 28 August 2013

Keywords:
Finite element
Local thermal non-equilibrium
Microwave ablation
Porous liver
Temperature distribution

ABSTRACT

Microwave ablation (MWA) is a process that uses the heat from microwave energy to kill cancer cells without damaging the surrounding tissue. The effectiveness of this technique is related to the temperature achieved during the process, as well as the input microwave power and heating time of treatment. The modeling of heat transport within biological tissues are key issues and have been used extensively in medical thermal therapeutic applications, for instance MWA treatment for predicting the temperature distribution during process. In this work, the interstitial MWA in porous liver by single slot microwave coaxial antenna (MCA) is carried out. A mathematical model of MWA of the porous media approach is proposed, which uses transient energy equation coupled with electromagnetic wave propagation equation to describe the temperature distribution within porous liver under local thermal non-equilibrium (LTNE) assumption. The LTNE assumption is taken into account by solving the two energy equations for tissue and blood phases. The thermal model considers the tissue with its blood vessel distribution as a porous medium and employs both the interfacial convective heat transfer and blood perfusion rate terms in the transient energy equations for both tissue and blood phases. The coupled nonlinear set of these equations is solved using the axisymmetric finite element method (FEM). The influences of blood velocities, porosities, input microwave powers and positions within the porous liver (distance from a MCA) on the tissue and blood temperature distributions have been investigated. Furthermore, the tissue and blood temperatures of LTNE model are compared with the tissue temperature of Pennes model and Klinger model. Through an accuracy comparison, the temperature results of the one-energy equation under local thermal equilibrium (LTE) model and Pennes model are compared with the experimental results from previous work in order to show the validity of the numerical results. The results show that the LTE assumption is found to be suitable for predicting the temperature distribution when the blood velocities to be 0.4 cm/s and 2 cm/s in all porosities, whilst, in case of blood velocities to be 3 cm/s and 3.4 cm/s the LTNE assumption for heat transfer analysis needs to be utilized. In addition, the LTE model is suitable for predicting a distribution of temperature when the high porosity for this model. This investigation provides the essential aspects for a fundamental understanding of heat transport within biological tissues while experiencing an applied electromagnetic field such as applications in the thermal ablation.

1. Introduction

Microwave ablation (MWA) techniques have become a extensive choice for the treatment of cancer, including liver, where the majority of the patients are not candidates for surgical resection due to restrictions, such as multifocal disease, tumor size, and position of tumor to key vessels. MWA can improve outcomes with few side effects [1] and also particularly useful when the tumor is located in an area that cannot be removed for functional purposes. The main advantages of MWA technology, when compared with existing thermal ablation technologies, include consistently higher intratumoral temperatures, larger tumor ablation volumes and faster ablation times [2]. In MWA treatments, the un-wanted tissue will be overheated to a therapeutic value, typically 50 °C to damage or kill the cancer cells and affect metastases [3]. The effectiveness of MWA process is related to the temperature achieved during the process. In order to kill cancer cells without damage to normal tissues, the ability to predict the temperature of the tumor and surrounding tissue is important in MWA. However, before real experimental cancer therapy, there should be basis numerical simulation. Therefore, the modeling of MWA in tissue is needed. The numerical simulation has important roles on the MWA

* Corresponding author. Tel.: +66 02 5643001 to 9x3153; fax: +66 02 5643023.
E-mail address: ratphadu@engr.tu.ac.th (P. Rattanadecho).

0017-9310/$ - see front matter © 2013 Elsevier Ltd. All rights reserved.
http://dx.doi.org/10.1016/j.ijheatmasstransfer.2013.07.064

Nomenclature

a	volumetric transfer area between the blood and the tissue (m^2/m^3)
C_p	specific heat capacity (J/(kg °C))
E	electric field (V/m)
f	microwave frequency (Hz)
H	magnetic field (A/m)
h	heat transfer coefficient (W/m^2 °C)
k	propagation constant (m^{-1})
K	thermal conductivity (W/(m °C))
P	input microwave power (W)
Q	heat source (W/m^3)
r	dielectric radius (m)
t	time (s)
T	temperature (°C)
u	blood velocity (cm/s)
Z	wave impedance in the dielectric of the coaxial cable (Ω)

Greek letters

μ	magnetic permeability (H/m)
ε	permittivity (F/m)
σ	electric conductivity (S/m)
λ	wave length (m)
ϖ	angular frequency (rad/s)
ω	blood perfusion rate (1/s)
ρ	density (kg/m^3)
ϕ	porosity (–)

Subscripts

b	blood
eff	effective
ext	external
inner	inner
met	metabolic
outer	outer
r	relative
r,*z*, and φ	components of cylindrical coordinates
s	solid
t	tissue
tb	tissue to blood
0	free space, initial condition

performance prediction in order to demonstrate the relationship between the microwave power deposited in the tissue and the resulting tissue status post treatment is highly complex, particularly in organs with high blood perfusion such as the liver. Furthermore, numerical simulation under various conditions can be studied for effective use in identifying the fundamental parameters as well as provide guidance for more realistic consideration in experiments.

In the past, the studies of MWA dealt with homogeneous material and focused on heat conduction (using Pennes's bioheat equation) within a medium. These models usually need many assumptions which may limit their applications in reality. Pennes's bioheat equation, introduced by Pennes [4] based on the heat diffusion equation, involves thermal conduction in tissue and vascular system, blood perfusion (through capillary tubes within the tissues) and also metabolic heat generation. The Pennes's bioheat models has been extensively used in many works for analysis of heat transfer in biological tissues, particularly in thermal ablation models [5–7]. Due to simplifications and shortcomings of this model, the Pennes's bioheat equation assumes the temperature of the blood within the capillaries equal to the body's core temperature. This means that all of the heat loss/gain occurs in the capillary bed and there are no losses or gains in the thermal energy of the blood in the higher order systemic components (large and intermediate sized vessels or veins) [8]. Therefore, other studies have investigated new models that substitute, modify the Pennes model model or coupled Pennes model with other models. For example, Klinger [9] developed a mathematical procedure which us to gain an exact analytical solution of the bioheat equation with convection terms. Yang et al. [10] proposed a new method to study high temperature tissue ablation using a modified bioheat equation to include tissue internal water evaporation during heating. The simulation result of modified bioheat equation is found in agreement well to the experimental result. After that Keangin et al. [11] carried out on the numerical simulation of liver cancer treated using the complete mathematical model considered the coupled model of bioheat model with electromagnetic wave propagation and mechanical deformation model in liver tissue during MWA process in the couple way.

In realistic, the biological tissue including cell and microvascular bed with the blood flow direction contains many vessels, assuming that the tissue is like a sponge, through which blood flows and can be regarded as a porous structure [12,13]. Thus, the study of heat transport in biological tissue should used porous media theory. The advantages of utilizing porous media theory in modeling of heat transfer is a fewer assumptions as compared to different established bioheat transfer models. Description of heat transport through porous media has been of interest for many decades. Two different models are used for analyzing heat transfer in a porous medium; local thermal equilibrium (LTE) and local thermal non-equilibrium (LTNE). Most of the prior works are based on invoking the LTE model based on the assumption that the tissue phase temperature is equal to fluid phase temperature everywhere in the porous medium. This assumption occurs when heat exchange between the tissue and the blood is efficient, it is a valid assumption in a capillary bed having many micro vessels (of small diameter) and a large area of heat transfer [14]. Explanation of the established LTE models can be found in the literature [15–18]. Alazmi and Vafai [15] investigated the effect of Darcy number, inertia parameter, Reynolds number, porosity, particle diameter, and the fluid-to-solid conductivity ratio on the velocity and temperature distributions within the porous media transport models. Later, Kou et al. [17] presented the effects of directional blood flow and heating schemes on the distributions of temperature and thermal dose during thermal therapy. A modified bioheat transfer equation based on the porous medium concept on LTE assumption by using a Green's function method was proposed to obtain the temperature distribution and thermal dose. The results showed that the domain of the thermal lesion might extend to the downstream normal tissue when the porosity and the averaged blood velocity are large. Recently, analyzed of heat transfer and blood flow on LTE assumption in two-layered porous liver tissue during MWA using single and double slot antenna was presented by Rattanadecho and Keangin [18]. The results show that the maximum specific absorption rate (SAR), temperature and blood velocity appears in the porous liver when using a single slot MCA is higher than when using a double slot antenna.

However, the LTE assumption is not valid for a number of physical situations such as when the fluid flows at a high speed through the porous medium [19]. Moreover, this assumption is not considered the temperature difference between the tissue and blood phases within the porous media. Which the temperature difference significantly influence on the heat transfer, especially during thermal ablation treatment. The criterion of LTE assumption during thermal ablation treatment may be different from that in the normal situation where metabolic heat source or external heat source occurs. In such cases, the LTNE assumption for heat transfer analysis needs to be utilized. This assumption based on heat transfer is convectively transferred between the two phases, making the two equations coupled. In recent years, the LTNE model in a porous medium has received more attention as demonstrated, such as Fan and Wang [20] developed a general bioheat transport model at macroscale for biological tissues based on porous media model. The model shows that both blood and tissue macroscale temperatures satisfy the derived the dual-phase-lag (DPL) energy equations. In the same year, Afrin et al. [21] presented a model of thermal lagging in living biological tissue based on LTNE heat transfer model between tissue, arterial and venous bloods. It was found that the phase lag times for heat flux and temperature gradient are the identical for the case that the tissue and blood have the same properties. Moreover, the LTNE model was used extensively in biomaterials during hyperthermia therapy [1,14,22–24]. Mahjoob and Vafai [22] analyzed characterization of heat transport through biological media incorporating hyperthermia treatment, utilizing the LTNE model of porous media theory, exact solutions for the tissue and blood temperature profiles were established. An equivalent heat transfer coefficient between tissue and blood in a porous model for simulating a biological tissue in a hyperthermia therapy based on the LTNE model was investigated by Yuan [23]. The results indicate that the equivalent heat transfer coefficient was not a strong function of the perfusion rate, blood velocity and heating conditions, but was inversely related to the blood vessel diameter. Next, Belmiloudi [24] analyzed the temperature distribution in biofluid heat transfer of porous non homogeneous tissues during thermal therapy based on LTNE model.

However, a few studies concentrated the heat transport of porous medium subjected to electromagnetic fields as in thermal ablation under LTNE model. Therefore, to approach reality, modeling of heat transport in porous tissue during thermal ablation is must be cooperating with the modeling of electromagnetic in order to completely these analysis. In addition, there are various effects related to the tissue and blood temperature, such as blood velocities, porosities and input microwave powers in a porous medium that still not well understood and several pertinent issues remain unresolved. The complete mathematical model is useful for the development of biomedical technologies especially.

In this study, investigates the transient distribution of tissue and blood temperatures within porous liver during MWA process using a single slot microwave coaxial antenna (MCA) based on LTNE model. Two equations of tissue and blood phases are used in the current study, to determine the implication of this new model for practical implementation. Mathematical model of MWA process of the porous media approach is proposed, which uses transient energy equation coupled with electromagnetic wave propagation equation. The coupled nonlinear set of governing equations as well as initial and boundary conditions are solved using the axisymmetric finite element method (FEM) via COMSOL^{TM} Multiphysics. The effect of blood velocities, porosities, input microwave powers and positions within the porous liver (distance from a MCA) in affecting the tissue and blood temperature distributions are analyzed. In order to verify the accuracy of the presented mathematical model of MWA, the resulting data of temperature from LTE model and Pennes model are validated against the experimental results, obtained by Yang et al. [10]. Furthermore, the tissue and blood temperatures of LTNE model are compared with the tissue temperature of Pennes model and Klinger model. The analysis from this study serves as essential fundament for the development of mathematic models of heat transfer for temperature prediction during MWA therapies that can be modified to present a more accurate temperature distribution within other biological tissues and can be used as a guideline for the practical treatment.

2. Problem Description

MWA is a process that uses the heat from microwave energy to kill cancer cells. The energy from the microwave frequency waves emitted by the microwave antenna creates heat in the local cancerous tissue cancer without the damaging surrounding tissue. This study uses a single slot MCA, to transfer microwave power into the porous liver for the treatment of liver cancer. The single slot MCA has a diameter of 1.79 mm, the thin antenna is required in the interstitial treatments because it is a minimally invasive and capable of delivering a large amount of electromagnetic power. A ring-shaped slot, 1 mm wide is cut off the outer conductor 5.5 mm in length from the short circuited tip because the effective heating around the tip of the antenna is very important to the interstitial heating and because the electric field becomes stronger near the slot [25]. The single slot MCA is composed of an inner conductor, a dielectric and an outer conductor. The single slot MCA is enclosed in a catheter (made of polytetrafluorethylene; PTFE), for hygienic and guidance purposes. Fig. 1 shows the model geometry of a single slot MCA. The single slot MCA operates at the frequency of 2.45 GHz, a widely used frequency in MWA, and the various input microwave powers. The goal of MWA is to elevate the temperature of un-wanted tissue (tumor) to 50 °C where cancer cells are destroyed [3]. Dimensions of a single slot MCA are given in Table 1. While the dielectric properties of a single slot MCA are given in Table 2.

In realistic, the structure of a tumor has been found to be different from that of normal tissue [26]. The structure of the tumors is very complicated. Therefore, the structures of tumor and normal tissue have been assumed to be the same in order to simplify the physical model to that of a uniform porous medium. In this study, the porous liver is considered as a cylindrical geometry. It has a 30 mm radius and 80 mm in height and a single slot MCA is inserted into the porous liver with 70.5 mm depth [11]. The vertical axis is oriented along the longitudinal axis of the single slot MCA, and the horizontal axis is oriented along the radial direction. The coaxial slot antenna exhibits rotational symmetry around the

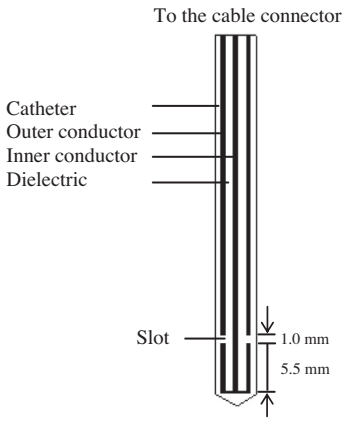

Fig. 1. Model geometry of a single slot MCA.

Table 1
Dimensions of a single slot MCA.

Materials	Dimensions (mm)
Inner conductor	0.135 (radial)
Dielectric	0.335 (radial)
Outer conductor	0.460 (radial)
Catheter	0.895 (radial)
Slot	1.000 (wide)

Table 2
The dielectric properties of a single slot MCA.

Properties	Relative permittivity ε_r	Electric conductivity σ (S/m)	Relative permeability μ_r
Dielectric	2.03	0	1
Catheter	2.1	0	1
Slot	1	0	1

longitudinal axis, therefore an axially symmetric model is considered in this study, which minimized the computation time while maintaining good resolution and represents the full three-dimensional result. Fig. 2 shows the axially symmetrical model geometry for analysis in this study. Three positions of the slot center are considered at p1 (2.5 mm, 16 mm), p2 (4.5 mm, 16 mm) and p3 (8.5 mm, 16 mm) to determine the tissue and blood temperatures.

In an anatomical view, biological tissues usually consist of three compartments, namely, blood vessels, cells and interstitial space [13,22]. The interstitial space can be further divided into the extracellular matrix and the interstitial fluid. However, for sake of simplicity, the biological tissues are divided into two distinctive regions, namely, the vascular region (blood vessels) and the extra-vascular region (cells and the interstitial space) and treat the whole anatomical structure as a blood saturated tissue represented by a porous medium [22], through which the blood infiltrates. The vascular region is regarded as a blood phase and extra-vascular region is regarded as a tissue (solid matrix) phase, as illustrated in Fig. 2. In this work, the tissue and blood local heat exchange, while the porous liver subjected to electromagnetic fields as in MWA process, is addressed and the tissue and blood temperature distributions are established analytically. Fundamental formulations of the governing equations based on LTNE model between the tissue (solid matrix) phase and blood phases within porous media have been presented in the literature [14,22,27].

The dielectric properties and thermal properties of the tissue and blood phases are assumed to be isotropic and constant are listed in Table 3 according to the study by Wessapan et al. [28] where the microwave frequency of 2.45 GHz is considered. Moreover, the heat transfer coefficient and blood velocity are assumed to be constant throughout the calculated domain.

Yuan [14] investigated the temperature and thermal dose response of biological tissue during hyperthermia therapy by using a range of porosities from 0.005 to 0.05. The range of porosities are corresponds to the capillaries, arterioles, terminal arteries, terminal branches, and tertiary branches. While, the range of porosities from 0.05 to 0.3 were selected for analyzed the heat transport through biological media incorporating hyperthermia therapy in work of Mahjoob and Vafai [22]. Therefore, a range of porosities from 0.025 to 0.1 are selected for investigating the tissue and blood temperature distributions within porous liver during MWA in this study. The relationship between blood velocity, porosity and volumetric transfer area between the blood and the tissue are given in Table 4 [14,29]. The blood velocity and volumetric transfer area are constant and are relevant to the different generations of the vasculature which taken from the literature [1,29].

3. The formulation of the mathematical model

In this section, an analysis of electromagnetic wave propagation and heat transfer within the porous liver during MWA process will be illustrated. The system of governing equations as well as initial and boundary conditions are solved numerically using the FEM via COMSOL^{TM} Multiphysics. The relevant boundary conditions are described in Fig. 3.

3.1. Equations for electromagnetic wave propagation analysis

This study investigates the transient temperature distribution within porous liver during MWA process. The microwave energy applied to the tumor causes water molecules to vibrate and rotate, resulting in heat to a temperature high enough to cause cell death. The electromagnetic wave propagation equation is solved for

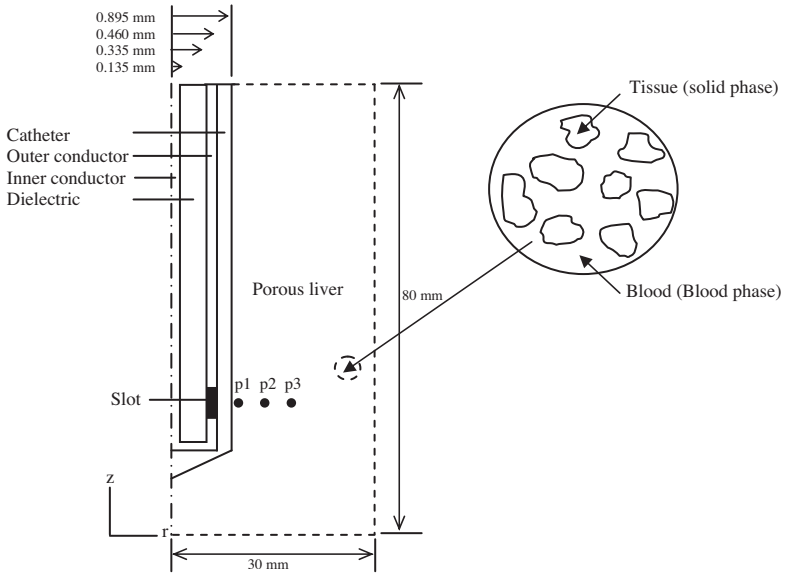

Fig. 2. Axially symmetrical model geometry. Three positions of the slot center are considered at p1 (2.5 mm, 16 mm), p2 (4.5 mm, 16 mm) and p3 (8.5 mm, 16 mm) to determine the tissue and blood temperatures.

Table 3
The thermal properties and dielectric properties of tissue and blood phases from Wessapan et al. [28].

Properties	Thermal conductivity K (W/m °C)	Density ρ (kg/m^3)	Specific heat capacity C_p (J/kg °C)	Relative permittivity ε_r	Electric conductivity σ (S/m)
Tissue phase (t)	0.497	1030	3600	43.00	1.69
Blood phase (b)	0.45	1058	3960	58.30	2.54

Table 4
The relationship between blood velocity, porosity and volumetric transfer area between the blood and the tissue [14,29].

Porosity (–)	Volumetric transfer area between the blood and the tissue (m^2/ m^3)			
	u = 0.4 cm/s	u = 2 cm/s	u = 3 cm/s	u = 3.4 cm/s
ϕ = 0.025	667	400	200	143
ϕ = 0.05	1333	800	400	286
ϕ = 0.1	6667	4000	2000	1429

microwave energy which is applied to porous liver during process. From the Fig. 2, this study is based on the following assumptions:

1. Electromagnetic wave propagation is modeled in 2D axially symmetrical cylindrical coordinates (r-z).
2. An electromagnetic wave, propagating in a MCA, is characterized by transverse electromagnetic fields (TEM) [30,31].
3. In the porous liver, an electromagnetic wave is characterized by transverse magnetic fields (TM) [30,31].
4. The model assumes that the wall of a MCA is a perfect electric conductor (PEC).
5. The outer surface of the porous liver is truncated by a scattering boundary condition.
6. The model assumes that dielectric properties of the porous liver are uniform and constant.

The axisymetric finite element (FE) model used in this study is adapted from a single slot MCA general model [10,32]. In this model, the electric and magnetic fields associated with the time-varying TEM wave are expressed in 2D axially symmetrical cylindrical coordinates:

$$\text{Electric field}(\vec{E}) \quad \vec{E} = e_r \frac{C}{r} e^{j(\varpi t - kz)} \tag{1}$$

$$\text{Magnetic field}(\vec{H}) \quad = e_\phi \frac{C}{rZ} e^{j(\varpi t - kz)} \tag{2}$$

where $C = \sqrt{\frac{ZP}{\pi . \ln(r_{outer}/r_{inner})}}$ is the arbitrary constant, Z is the wave impedance(Ω), P is the input microwave power (W), r_{inner} is the dielectric inner radius (m), r_{outer} is the dielectric outer radius (m), $\varpi = 2\pi f$ is the angular frequency (rad/s), f is the frequency (Hz), k is the propagation constant (m^{-1}) which relates to the wave length (λ) in the medium (m); $k = \frac{2\pi}{\lambda}$.

In the porous liver, the electric field also has a finite axial component, whereas the magnetic field is purely in the azimuth direction. The electric field is in the radial direction only inside the coaxial cable and in both radial and the axial direction inside the tissue. This allows for a single slot MCA to be modeled using an axisymmetric TM wave formulation. The wave equation then becomes scalar in H_ϕ:

$$\nabla \times \left(\left(\varepsilon_r - \frac{j\sigma}{\omega \varepsilon_0} \right)^{-1} \nabla \times \vec{H}_\phi \right) - \mu_r k_0^2 \vec{H}_\phi = 0 \tag{3}$$

where $\varepsilon_0 = 8.8542 \times 10^{-12}$ F/m is the permittivity of free space, ε_r is the relative permittivity, σ is the electric conductivity (S/m), μ_r is the relative permeability and k_0 is the free space wave number (m^{-1}).

3.1.1. Boundary condition for electromagnetic wave propagation analysis

Microwave energy is emitted from the MCA slot, which connected to the microwave generator, and propagates through the MCA into the porous liver from the MCA slot. Therefore, boundary condition for analyzing electromagnetic wave propagation, as shown in Fig. 3, is considered as follows:

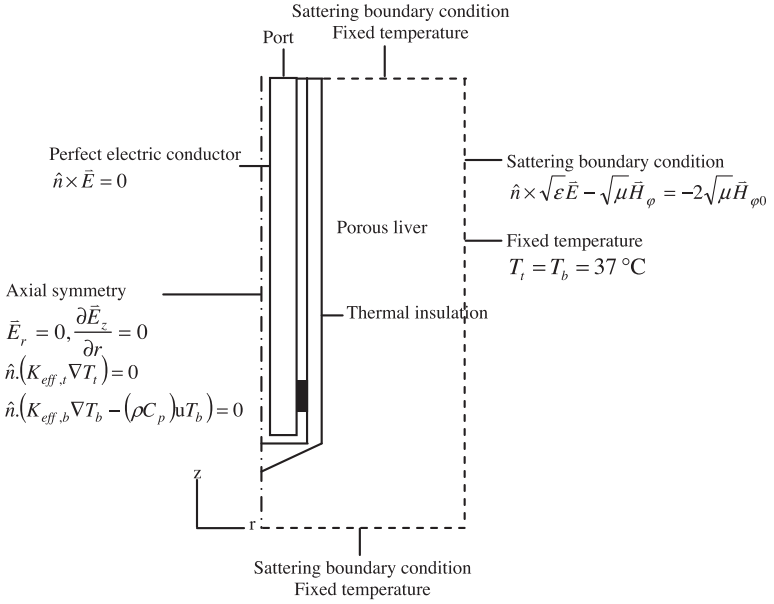

Fig. 3. Boundary condition for analysis of electromagnetic wave propagation and heat transfer.

At the inlet of the MCA, TM wave propagation with various input microwave powers is considered. An axial symmetry boundary is applied at $r = 0$:

$$\vec{E}_r = 0 \tag{4}$$

$$\frac{\partial \vec{E}_z}{\partial r} = 0 \tag{5}$$

The first order scattering boundary conditions for $\vec{H}_\phi$ were used along the outer sides of the porous liver boundaries to prevent reflection artifacts [11]:

$$\hat{n} \times \sqrt{\varepsilon}\,\vec{E} - \sqrt{\mu}\vec{H}_\phi = -2\sqrt{\mu}\vec{H}_{\phi 0} \tag{6}$$

where $\vec{H}_{\phi 0} = C/Zr$ is the excitation magnetic field.

For simplicity and to eliminate numerical error, the inner and outer conductors of the MCA are modeled as the PEC boundary conditions:

$$\hat{n} \times \vec{E} = 0 \tag{7}$$

3.2. Equations for heat transfer analysis

In analysis of heat transfer, the tissue and blood temperatures within the porous liver during MWA process are obtained by solving the two energy equations under LTNE assumption where the microwave power absorbed is included. The temperature distribution corresponds to the microwave power absorbed. This is because when microwave propagates in the porous liver, microwave energy is absorbed by the porous liver and converted into internal heat generation which causes the porous liver temperature to rise. To simplify the problem, the following assumptions are made:

1. Corresponding to electromagnetic wave propagation analysis, blood flow and heat transfer analysis in the liver is assumed in 2D axially symmetrical cylindrical coordinates (r–z).
2. The porous liver is considered homogenous, thermally isotropic and is saturated with a fluid (blood).
3. The blood flow is an incompressible and Newtonian [13,20].
4. There is no phase change occurs within the porous liver, no energy exchange through the outer surface of the porous liver, and no chemical reactions occur within the porous liver.
5. The porosities and thermal properties of the porous liver are assumed to be constant.

The transient temperature distribution within the porous liver is obtained by solving the energy equations of tissue and blood phases where the microwave power absorbed and an internal heat sources (namely metabolic heat source) are included. However, the metabolic heat source includes only in tissue phase energy equation [13,22,27]. The governing equations describing the heat transfer phenomenon for tissue and blood phases incorporating with LTNE conditions can be represented as [27]:

Tissue phase:

$$(1-\phi)(\rho C_p)_t \frac{\partial T_t}{\partial t} = \nabla \cdot (K_{t,eff} \nabla T_t) - h_{tb} a_{tb}(T_t - T_b) - \omega_b C_b \times (T_t - T_b) + (1-\phi) Q_{met} + (1-\phi) Q_{ext,t} \tag{8}$$

Blood phase:

$$\phi(\rho C_p)_b \left(\frac{\partial T_b}{\partial t} + \mathrm{u} \cdot \nabla T_b \right) = \nabla \cdot (K_{b,eff} \nabla T_b) + h_{tb} a_{tb}(T_t - T_b) + \omega_b C_b (T_t - T_b) + \phi Q_{ext,b} \tag{9}$$

where

$$K_{t,eff} = (1-\phi) K_t \tag{10}$$

$$K_{b,eff} = \phi K_b \tag{11}$$

where subscripts *eff*, *t* and *b* represent the effective value, tissue and blood phase, respectively, T is the temperature averaged (°C), ρ is the density (kg/m^3), C_p is the specific heat capacity (J/kg °C), K is the thermal conductivity (W/m °C), ϕ is the porosity which is the ratio of the blood volume to the total volume (–) [13], u is the blood phase average velocity (cm/s), ω is the blood perfusion rate (1/s), h_{tb} is the blood to tissue interfacial heat transfer coefficient (W/m^2 °C) and a_{tb} is thevolumetric transfer area between the blood and the tissue (m^2/m^3). The h_{tb} depends on the nature of the porous matrix and the saturating fluid and the value of this coefficient has been the subject of intense experimental interest. Large values of h_{tb} correspond to a rapid transfer of heat between the phases (LTE assumption) and small values of h_{tb} gives rise to relatively strong LTNE effects [33]. In this study, the blood to tissue interfacial heat transfer coefficient is selected to be 170 W/m^2 °C for all cases [14].

From the Eq. (8), the first, second, third, fourth and fifth terms on the right-hand side of equation denote heat conduction term, interstitial convection heat transfer term, blood perfusion term, metabolic heat source and external heat source (heat generation by the electric field), respectively. On the other hand, the first and second terms on the left-hand side of Eq. (9) denotes the transient term and convection term due to blood flow, respectively. While, bulk blood flow term appears on the left side of the blood phase energy equation (Eq. (9)), as part of the total temporal derivative.

As seen from two energy equations for tissue and blood phases are coupled by the interstitial convective heat transfer term and blood perfusion term. The interstitial convective heat transfer term and blood perfusion term are different processes and should not be confused [13]. The blood perfusion term is the process of nutritive delivery of arterial blood to a capillary bed in the biological tissue [27]. The temperature of the blood is decreased from T_b to T_t in the perfusion process and the energy change in this process. The blood perfusion term is added in both tissue and blood phases, accounting for the heat transfer associated with the transcapillary fluid exchange via arterial-venous anastomoses that was included in Nakayama and Kuwahara [13] and Zhang [27]. In this study, the blood perfusion rate is selected to be 0.0036 1/s for all cases [34]. On the other hand, the interstitial convective heat transfer term is the process of the temperature changes as result of convective heat transfer between the blood and the peripheral tissues. The effects of vascular geometry and size can also be accounted for by blood to tissue interfacial heat transfer coefficient (h_{tb}) and the volumetric transfer area between the blood and the tissue (a_{tb}).

The metabolic heat source (Q_{met}) is 33,800 W/m^3 [35,36], while the external heat source (Q_{ext}) is equal to the resistive heat generated by electric field and can be defined as [37]:

$$Q_{ext} = \frac{\sigma |\vec{E}|^2}{2} \tag{12}$$

When LTE assumption is maintained, the temperature of the tissue is equal to that of the blood temperature ($T_t = T_b = T$). Therefore, the above Eqs. (8) and (9) can be combined into a one equation as follows:

$$((1-\phi)(\rho C_p)_t + \phi(\rho C_p)_b) \frac{\partial T}{\partial t} + \phi(\rho C_p)_b (\mathrm{u} \cdot \nabla T) = \nabla \cdot ((1-\phi) K_t + \phi K_b) \nabla T + (1-\phi) Q_{met} + Q_{ext} \tag{13}$$

The Pennes's bioheat equation which the metabolic heat source and the external heat source are applied to the tissue can be written as [28,31]:

$$(\rho C_p)_t \frac{\partial T_t}{\partial t} = \nabla \cdot (K_t \nabla T_t) + (\rho C_p)_b \omega_b (T_b - T_t) + Q_{met} + Q_{ext} \quad (14)$$

where T_b is the blood temperature and is assumed to be uniform throughout the tissue, normally taken as body temperature 37 °C [18]. Eq. (14) is one of the earliest heat transfer equations that describes the temperature distribution in biological tissue. The blood perfusion effect is assumed to be homogeneous and isotropic, i.e., the effect of directional blood flow cannot be described by the Pennes's bioheat equation.

The Klinger model with the assumption of quasi-steady state [1]:

$$(\rho C_p)_t \frac{\partial T_t}{\partial t} + \phi (\rho C_p)_b (\mathrm{u}.\nabla T) = \nabla \cdot (K_t \nabla T_t) + Q_{met} + Q_{ext} \quad (15)$$

The main difference between Eq. (14) and Eq. (15) is found in their convection term due to blood flow, this term in Eq. (15) accounts for the directional effect of blood flow on the tissue temperature distribution, whilst, that of Eq. (14) acts as a blood perfusion term.

3.2.1. Boundary condition for heat transfer analysis

The heat transfer analysis under LTNE assumption is considered only in the porous liver, which does not include the MCA. As shown in Fig. 3, the boundaries of porous liver corresponds to the assumption are considered as follows:

An axial symmetry boundary is applied at $r = 0$ for the heat transfer analysis:

$$\hat{n} \cdot (K_{eff,t} \nabla T_t) = 0 \quad (16)$$

$$\hat{n} \cdot (K_{eff,b} \nabla T_b - (\rho C_p)_b \mathrm{u} T_b) = 0 \quad (17)$$

At the outer surface between the MCA and the porous liver is considered as adiabatic boundary condition. While, the tissue and the blood temperatures at surroundings of the porous liver will be the same at fixed temperature at 37 °C

$$T_t = T_b = 37\,^{\circ}C \quad (18)$$

The initial temperature of the porous liver is assumed to be uniform:

$$T(t_0) = 37\,^{\circ}C \quad (19)$$

4. Numerical simulations

In this study, the FEM is used to analyze the transient problems. The computational scheme is to assemble axisymmetric FEM model with suitable time and spatial step size. The coupled model of electromagnetic wave propagation and heat transfer analysis are solved by the FEM, to demonstrate the phenomenon that occurs within the porous liver during MWA. Analysis of heat transfer can be modeled by solving a conjugate problem containing a tissue and blood phases. Both initial tissue and blood temperatures are set to be body temperature 37 °C at the beginning of the ablation. The computational scheme starts with computing an external heat source term by running an electromagnetic wave propagation calculation and subsequently solves the time dependent temperature in the porous liver. All the steps are repeated until the required heating time is reached.

The description of heat transfer pattern, Eqs. (8)–(11), (13)–(19) requires specification of tissue temperature (T_t) and blood temperature (T_b). These equations are coupled to the electromagnetic wave propagation equations Eqs. (1)–(7) and energy equation by Eq. (12). The time-steps used to solve the system of equations describing electromagnetic wave propagation and heat transport are $\Delta t = 2 \times 10^{-12}$ s and $\Delta t = 0.01$ s, respectively.

The axisymmetric FEM model is discretized using triangular elements with the Lagrange quadratic shape functions. In order to obtain a good approximation, a fine mesh has been generated in the vicinity of the tip of the antenna, where the temperature is more concentrated. The set of partial differential equations along with their related boundary conditions are coupled and are solved numerically by the FEM via COMSOL™ multiphysics. FEM models can provide users with quick, accurate solutions to multiple systems of differential equations and as such, are well suited to heat transfer problems like ablation [30]. The system of governing equations as well as initial and boundary conditions are solved with the Unsymmetric Multifrontal Method (UMFPACK) solver to approximate tissue and blood temperatures variation across each element. The predicted tissue temperature of the Pennes model and the Klinger model, with the same model parameters and the same initial and boundary conditions as the LTNE model, are also simulated in three blood velocity cases to provide a direct comparison. The convergence test is carried out to identify the suitable numbers of element required. The convergence curve resulting from the convergence test is shown in Fig. 4. This figure shows the relationship between temperature and number of elements from simulations at a critically sensitive point, of the slot center (insertion depth of 64 mm). This convergence test leads to a grid with approximately 20,471 elements. It is reasonable to confirm that, at this number of element, the accuracy of the simulation results is independent from the number of elements through the calculation process. Cases with higher numbers of elements are not tested due to a lack of computational memory and performance.

5. Results and discussion

In this analysis, the influences of blood velocities ($u = 0.4$, 2, 3 and 3.4 cm/s), porosities ($\phi = 0.025$, 0.05 and 0.1), input microwave power ($P = 5$, 10, 15, 20 W) and positions within the porous liver (distance from MCA) (p1 (2.5 mm, 16 mm), p2 (4.5 mm, 16 mm) and p3 (8.5 mm, 16 mm)) on distributions of tissue and blood temperatures within the porous liver are systematically investigated. A parametric study has been carried out to assess the effect of each of these factors separately and analyze their contributions in determining the tissue and blood temperature distributions.

5.1. Validation of the model

It must be noted in advance that it is very difficult to make direct comparison of the model in this study and the experimental results because it is not possible to directly measure the temperature increase in the liver tissue, especially in the case where electromagnetic field is effected during MWA ablation is taken into account. In order to verify the accuracy of the presented mathematical model, the simulation results of tissue temperature of the porous liver based on LTE model and tissue temperature of bioheat model are then validated against the experimental results with the same geometric model and the same testing condition obtained by Yang et al. [10]. The geometry of the validation case as shown in Fig. 5. In the validation case, the input microwave power of 75 W with frequency of 2.45 GHz and the initial liver tissue temperature of 8 °C are used. The single slot MCA with a radius of 1.25 mm is inserted into liver tissues 20 mm in depth. The axially symmetrical model is used to analyze the MWA process with the heating time of 50 s. The validation results of the selected test case are illustrated in Fig. 6 for temperature distribution in the liver tissue, with respect to the heating time of 50 s with the positions of 4.5 mm and 9.5 mm away from the MCA. From the figures, it can be observed that the simulated results of the tissue temperature of the porous liver based on LTE model corresponds well to the

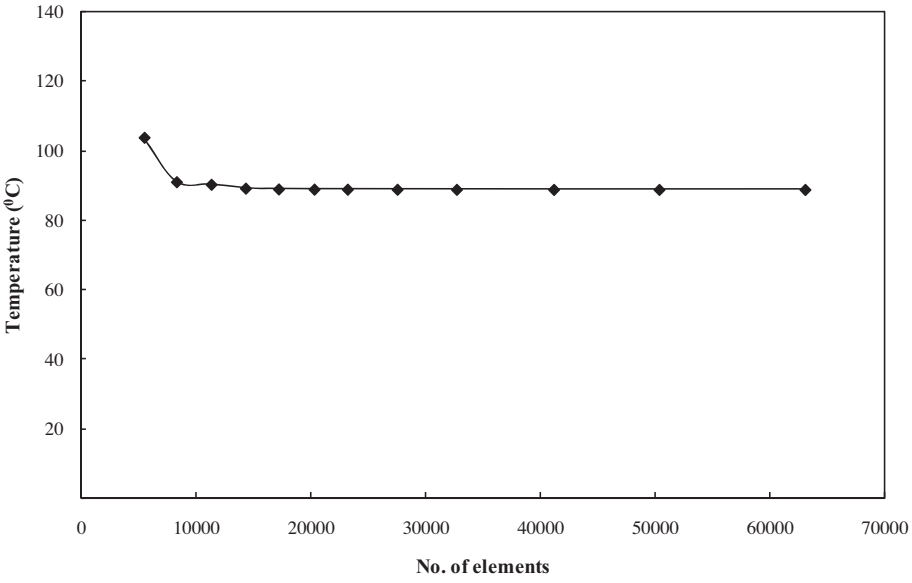

Fig. 4. Grid convergence curve of the model.

experimental results with similar trends in temperature distribution over the same approximate time range at both positions, especially at the end stage. This is due to the fact that the porous media model is based on convective heat mode coupled with conduction heat mode. While the bioheat model is manly governed by conduction heat mode. Considering the fact that the convective heat is influence increases at the end stage, it is obvious that the porous media model yields better results. Table 5 shows the comparisons of the root mean square error (RMSE) of the liver tissue temperature between the tissue temperature from LTE model and tissue temperature from bioheat model in present study with experimental data obtained from Yang et al. [10]. From the table, it is observed that the bioheat model gives greater error than the simulated temperature obtained from porous media model. However, at the position of 9.5 mm away from the MCA, the temperature distribution match the experimental results better than the temperature distribution at the position of 4.5 mm. Therefore, the selected developed model based on porous media approach is reasonable and can be used effectively for this problem. This is important to obtain the approaching realistic tissues modeling during MWA.

Although the simulation result of temperature based on LTE model agree well with the experimental data obtained from Yang et al. [10], the LTE model is not considered the temperature difference between the tissue and blood phases within the biological tissue that significant in to heat transfer, especially during thermal ablation treatment. Therefore, the analysis of heat transport in biological tissue during thermal ablation should consider the LTNE model. These simulated results will contribute to a greater clarity concerning attributes more closely to actual behavior of thermal ablation.

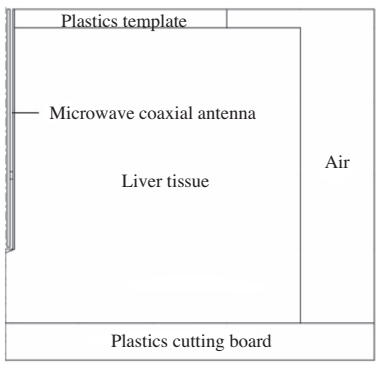

Fig. 5. Geometry of the validation model obtained from the Yang et al. [10].

5.2. Comparison of tissue and blood temperature of LTNE model and tissue temperature of Pennes model and Klinger model

The prediction of tissue and blood temperature distributions within the porous liver is crucial for an effective MWA therapy. The tissue and blood temperature distributions obtained from the numerical simulation correlations effectively address this need.

Fig. 7 depicts the simulation results of temperature distribution the center of the slot exit (z = 16 mm) versus models at three positions based on P = 10 W, f = 2.45 GHz, ϕ = 0.05, u = 2 cm/s and t = 300 s. Fig. 7(a) and (b) shows the tissue and blood temperature distributions of the LTNE model, respectively. While, Fig. 7(c) and (d) shows the tissue temperature distribution of the Pennes model and Klinger model, respectively. It can seen that the tissue and blood temperature distributions of the LTNE model and the tissue temperature distribution of the Pennes model have similar trends with a slight difference in magnitude. The distribution of temperature in three cases are increases with an increases in heating time. Therefore, the predicted tissue temperature distribution pattern of the Pennes model (Fig 7(c)) is shown to be almost identical to that of the that tissue and blood temperature distributions of the LTNE model, whilst, the parallel simulated temperature distribution pattern of the Klinger model (Fig. 7(d)) is, in contrast, very different. This demonstrates that the Pennes model is much closer in equivalence to the tissue and blood temperature distributions of LTNE model in case of blood velocity to be 2 cm/s. Consider the different of tissue and blood temperature distributions from LTNE model, it is found that the pattern of temperature distribution are very similar trends. It can be concluded that the LTE model is suitable for a predicted the distribution of temperature when the blood velocity to be 2 cm/s for this condition.

Fig. 8 illustrates the simulation results of temperature distribution the center of the slot exit (z = 16 mm) versus models at three positions based on P = 10 W, f = 2.45 GHz, ϕ = 0.05, u = 3.4 cm/s and t = 300 s. Fig. 8(a) and (b) shows the tissue and blood temperature distributions of the LTNE model, respectively. While, Fig. 8(c) and (d) shows the tissue temperature distribution of the Pennes model

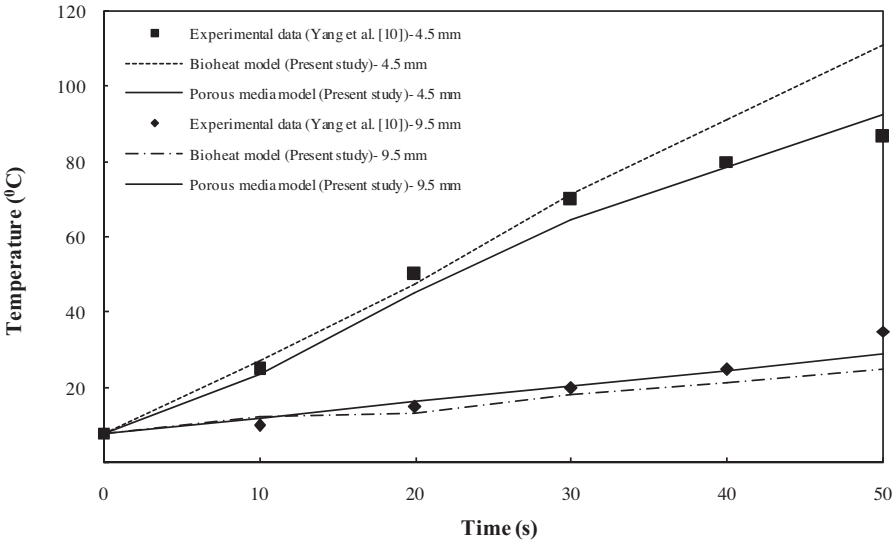

Fig. 6. The validation results of tissue temperature of the porous liver based on LTE model and tissue temperature of bioheat model, against the experimental results obtained by Yang et al. [10].

Table 5
Comparisons of RMSE of the liver tissue temperature between the present study and Yang et al. [10].

Position (mm)	Comparisons of RMSE with experimental data obtained from Yang et al. [10] (°C)	
	Bioheat model (present study)	Porous media model (present study)
4.5 mm	11.10	3.87
9.5 mm	4.52	2.73

and Klinger model, respectively. It can observed that the tissue temperature distribution (Fig. 8(a)) and the blood temperature distribution (Fig. 8(b)) are significantly different, especially at position of p1. Due to this position is close to the MCA that hot spot zone occurs. This demonstrates that the LTE model is not suitable for a predicted the distribution of temperature, suggesting the importance of utilizing the LTNE model when the blood velocity to be 3.4 cm/s for this condition. Referring to Table 4, at blood velocity to be 3.4 cm/s is lower the volumetric transfer area between the blood and the tissue as a result of lower heat exchange between two phases in all porosities, therefore, it can conclude that a low heat exchange lead to a large difference between the tissue and blood temperatures. A similar conclusion has been achieved by Peng et al. [1] and Mahjoob and Vafai [22] when studying the heat transport through biological media. Although the tissue temperature distribution of the Pennes model Fig. 8(c) has similar trends with a tissues temperature distribution of the LTNE model (Fig. 8(a)), a difference in magnitude. While, the simulated temperature of Klinger model (Fig. 8(d)) is also in contrast from the other models corresponds to the results in Fig. 7.

5.3. Comparison of tissue and blood temperature profiles of LTNE model and tissue temperature profile of LTE model

The comparison of tissue and blood temperature profiles of LTNE model and tissue temperature profile of LTE model within the porous liver for heating times of 60 s, 180 s, and 300 s based on $P = 10$ W, $f = 2.45$ GHz, $\phi = 0.05$ and $u = 3.4$ cm/s, are shown in Fig. 9. In all cases, the temperature profile forms a nearly ellipsoidal shape around the slot and the highest value occurs in the vicinity of the slot MCA and decreases with the distance from the MCA. Moreover, the temperature profile in three cases are increases with an increases in heating time. It is interesting to observe that the temperature of tissue and blood from LTNE models and the temperature of tissue from LTE models that far from the MCA are found to be close to the initial temperatures 37 °C. By comparison between tissue and blood temperature profile from LTNE models, it is clear that the difference of temperature profile pattern with a slight difference in magnitude at all heating times. The comparison between the maximum temperatures in three cases, it can be seen that the maximum tissue temperature of LTNE model has a higher maximum temperatures value within the porous liver than that of the maximum blood temperature of LTNE model and maximum tissue temperature of LTE model, respectively at all duration times. The maximum temperature differences for the temperature of tissue and blood from LTNE models are 0.514% and the maximum temperature differences for the temperature of tissue from LTNE and LTE models are 4.167%, respectively at the end of process. Although the patterns of temperature profile of tissue from LTNE is similar to the temperature profile of tissue from LTE models, the maximum temperature values are quite different. Therefore, the LTNE assumption for heat transfer analysis needs to be utilized for this condition.

5.4. Effect of porosity

During thermal ablation treatments, the porosities is likely to change as a part of the natural body temperature regulation system [22]. The natural cooling system in the body, the blood regulates the body temperature during thermal ablation by arterial blood with the cold body core temperature, while modifying the porosity of the biological structure. The natural body thermal regulation system increases or decreases the porosity of the biological structure when exposed to a higher or lower temperature, respectively. A change in the porosity also translates in a change in the and blood and effective thermal conductivities as shown in Eqs. (10) and (11). Therefore, the investigation of the effect of porosities on the temperature distribution may have large practical significance. In this section discusses the effect of porosities on the tissue and blood temperature distributions.

Fig. 10 shows the tissue and blood temperature distributions of the LTNE model versus time for different blood velocities at the position p1 ($r = 2.5$ mm, $z = 16$ mm) based on $P = 10$ W, $f = 2.45$ GHz, $\phi = 0.1$ and $t = 300$ s. In this figure, the difference be-

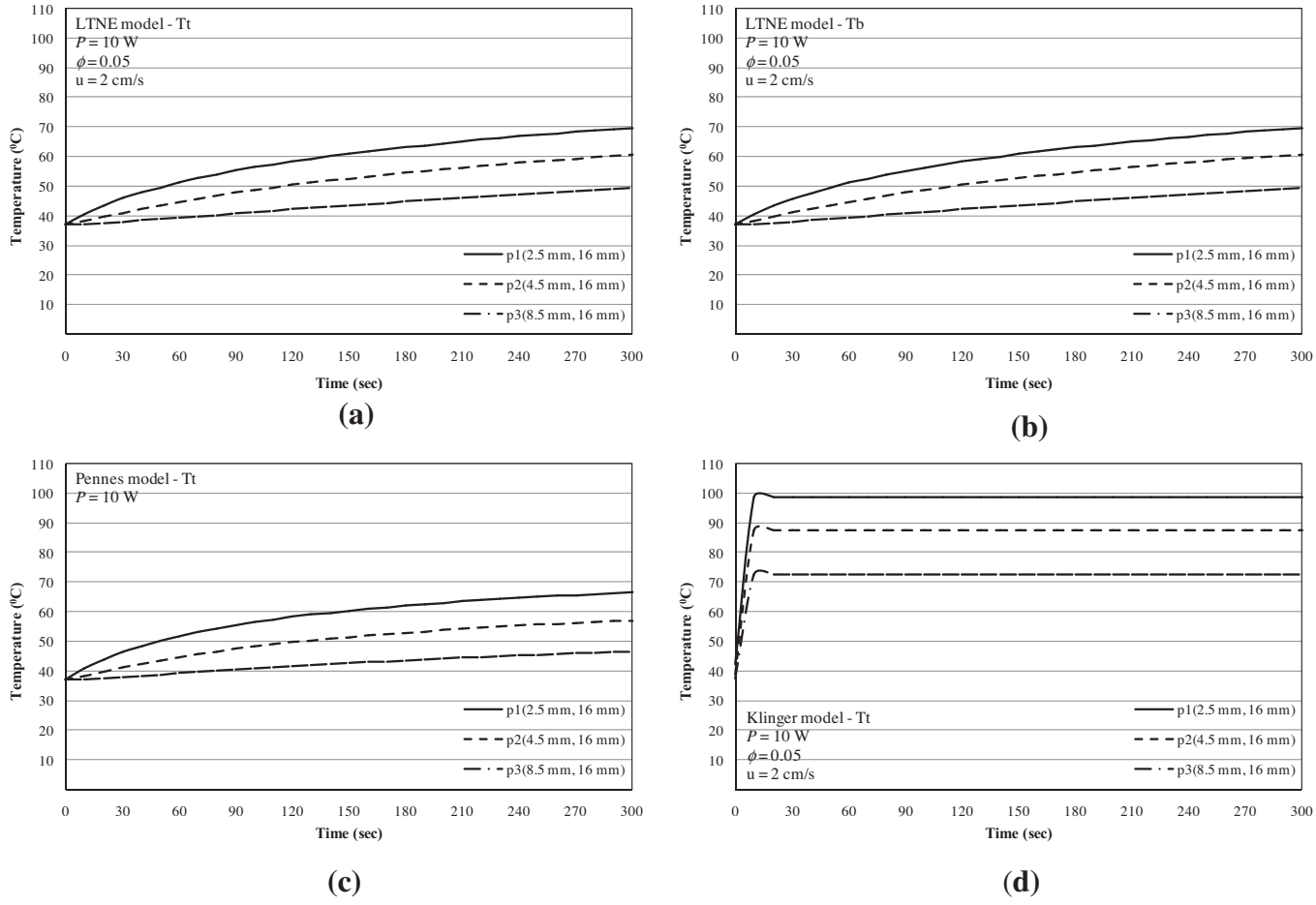

Fig. 7. The temperature distribution at the center of the slot exit (z = 16 mm) versus models (a) and (b) tissue and blood temperature distributions of the LTNE model; (c) tissue temperature distribution of the Pennes model and (d) tissue temperature distribution of the Klinger model, respectively at three positions; (P = 10 W, f = 2.45 GHz, ϕ = 0.05, u = 2 cm/s and t = 300 s).

tween tissue and blood temperature distributions hardly varies for the same blood velocities when the porosity to be 0.1. The distribution of tissue and blood temperatures of all blood velocities are increases with an increases in heating time. Therefore, it can be concluded that the LTE assumption is suitable for a predicted the distribution of temperature when the porosity to be 0.1 for this condition. Consider the effect of blood velocity on the tissue and blood temperature distributions, it is found that the lower blood velocity provides a higher tissue and blood temperature distributions within the porous liver. This is because the lower blood velocity have a higher internal heat exchange, as given in Table 4 results in a higher tissue and blood temperatures.

The effect of lower porosity (ϕ = 0.05) on tissue and blood temperature distributions of the LTNE model versus time for different blood velocities are illustrates in Fig. 11. From the Fig. 11, it is can seen that the tissue and blood temperature distributions in Fig. 11 are similar trends to the tissue and blood temperature distributions in Fig. 10. The distribution of temperature of two phases increases with an increases in heating time. The tissue and blood temperature distributions have similar trends in case blood velocity to be 0.4 cm/s and 2 cm/s. On the other hand, the tissue temperature distribution is different from blood temperature distribution in case blood velocity to be 3 cm/s and 3.4 cm/s. Which the tissue temperature distribution is different from blood temperature distribution in case blood velocity to be 3.4 cm/s more than that in case blood velocity to be 3 cm/s when the porosity to be 0.05 is used. This implies that the LTE assumption is suitable for in case blood velocity to be 0.4 cm/s and 2 cm/s at the porosity to be 0.05. In Eq. (9), the second term on the left of the equation represents the convection heat transferred out by the blood flow, and it depends on the porosity, blood properties, blood velocity, and temperature gradient. When the blood velocity in the tissue is low, the porous medium easily approaches the LTE assumption of equal temperatures of the tissue and blood because of an increase in the internal heat exchange between the tissue and blood. Besides, the comparison of tissue and blood temperatures within porous liver, it is can observed the blood temperature must be lower than the tissue temperature due to the different microwave power absorbed of tissue and blood during the MWA process. That the microwave power absorbed of blood is less than that of tissue during thermal therapy [38].

Fig. 12 depicts the tissue and blood temperature distributions of the LTNE model versus time for different blood velocities with ϕ = 0.025. In Fig. 12, it is clear that the LTE assumption is suitable for blood velocity to be 0.4 cm/s and 2 cm/s when the porosity to be 0.025 due to the tissue temperature match with the blood temperature. While, the difference between the temperature of two phases can see clearly in case blood velocity to be 3 cm/s and 3.4 cm/s. Moreover, the difference between the temperature of two phases with blood velocity to be 3 cm/s and 3.4 cm/s when the porosity to be 0.025 in Fig. 12 is higher than the difference between the temperature of two phases in same two blood velocities when the porosity to be 0.05 in Fig. 11.

Referring to the simulation result in Figs. 10–12, the tissue temperature match the result of blood temperature with blood velocity

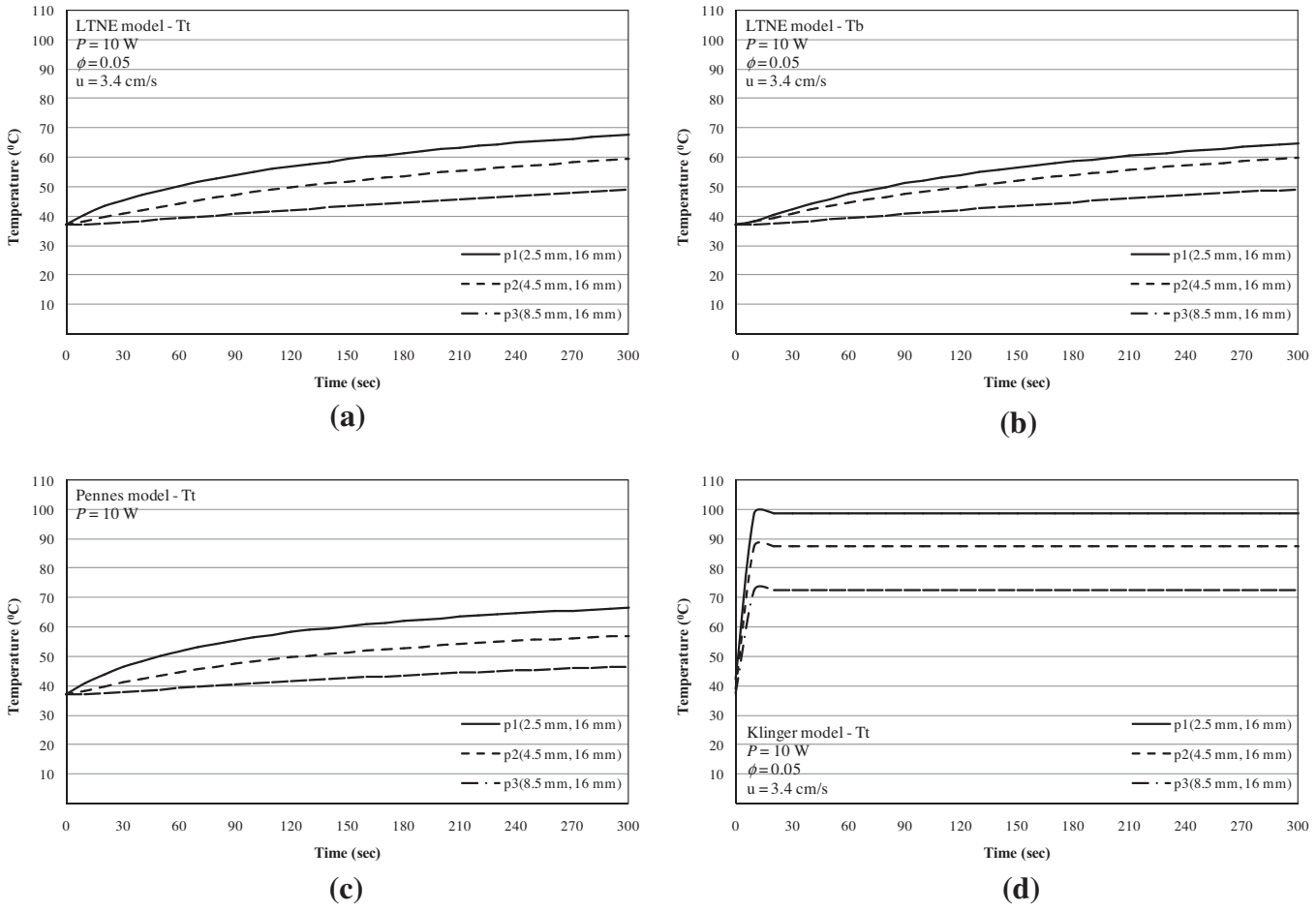

Fig. 8. The temperature distribution at the center of the slot exit (z = 16 mm) versus models (a) and (b) tissue and blood temperature distributions of the LTNE model; (c) tissue temperature distribution of the Pennes model and (d) tissue temperature distribution of the Klinger model, respectively at three positions; (P = 10 W, f = 2.45 GHz, ϕ = 0.05, u = 3.4 cm/s and t = 300 s).

to be 0.4 cm/s and 2 cm/s in every conditions. This show that the LTE assumption is valid for all porosities used in this study when blood velocity to be 0.4 cm/s and 2 cm/s. On the other hand, when blood velocity to be 3 cm/s and 3.4 cm/s the LTNE assumption for heat transfer analysis needs to be utilized. Because the difference of temperature in two phase varies significantly.

Furthermore, referring to the literature [1,14,29], the vasculature with a large blood velocity (blood velocities are 3 cm/s and 3.4 cm/s) will has a larger vessel diameters than that the small blood velocity (blood velocities are 0.4 cm/s and 2 cm/s). Therefore, from the result in the Figs. 10–12, can provides an alternative way to estimate the analysis of heat transport of the whole vasculature during thermal ablation. For the analysis of heat transport in biological media including multiple vessel types, the temperature of a large vessel diameters should be calculated directly from the LTNE assumption, while the heat transport of small vessel diameters or the microvasculature may be neglected because they are completely thermally equilibrated with the surrounding tissue.

Because of the difference in tissue and blood temperatures is the most obvious with blood velocity is 3.4 cm/s, Fig. 13 explains the comparison of the tissue and blood temperature distributions of the LTNE model versus time for different porosities at the position p1 (r = 2.5 mm, z = 16 mm) at blood velocity is 3.4 cm/s. When the porosities is large (ϕ = 0.1), there is little difference between the tissue and blood temperatures, in which case the model prediction could be approximated by that of LTE model. Because higher porosity implies having more blood to carry the heat away from the tissue, consequently the tissues temperature to be close to the blood temperature. The temperature uniformity can be achieved within a biological structure with a larger porosity resulting in a more effective thermal treatment [22]. On the other hand, the larger difference between the tissue and blood temperatures when an decrease in the porosities (ϕ = 0.05 and 0.025) completely breaks down the LTE assumption between the tissue temperature and the blood temperature are better approximated by the assumption of LTNE. Due to a higher porosity leads to a lower microwave power absorbed, hence the time-varying tissue and blood temperature distributions of higher porosity are lower than those of lower porosity the heating duration time and blood velocity maintain the same input.

5.5. Effect of input microwave power

In this section, discusses the effect of input microwave power on tissue and blood temperatures of LTNE model. The input microwave powers of 5 W, 15 W and 20 W are selected for study and demonstration. These input microwave powers are selected during MWA in order to estimate the appropriate power setting of MWA applied treatment for liver cancer. While, the effect of input microwave power is 10 W on tissue and blood temperatures of LTNE model can be seen in the section of 5.4. In addition, the porosity of 0.025 and blood velocity of 3.4 cm/s are selected in this section due to in this condition it is clear that the difference of tissue and blood temperatures. With regard to the tissue and blood temperatures at the three positions are shown in Fig. 2. Fig. 14 shows the tissue and blood temperature distributions of the LTNE

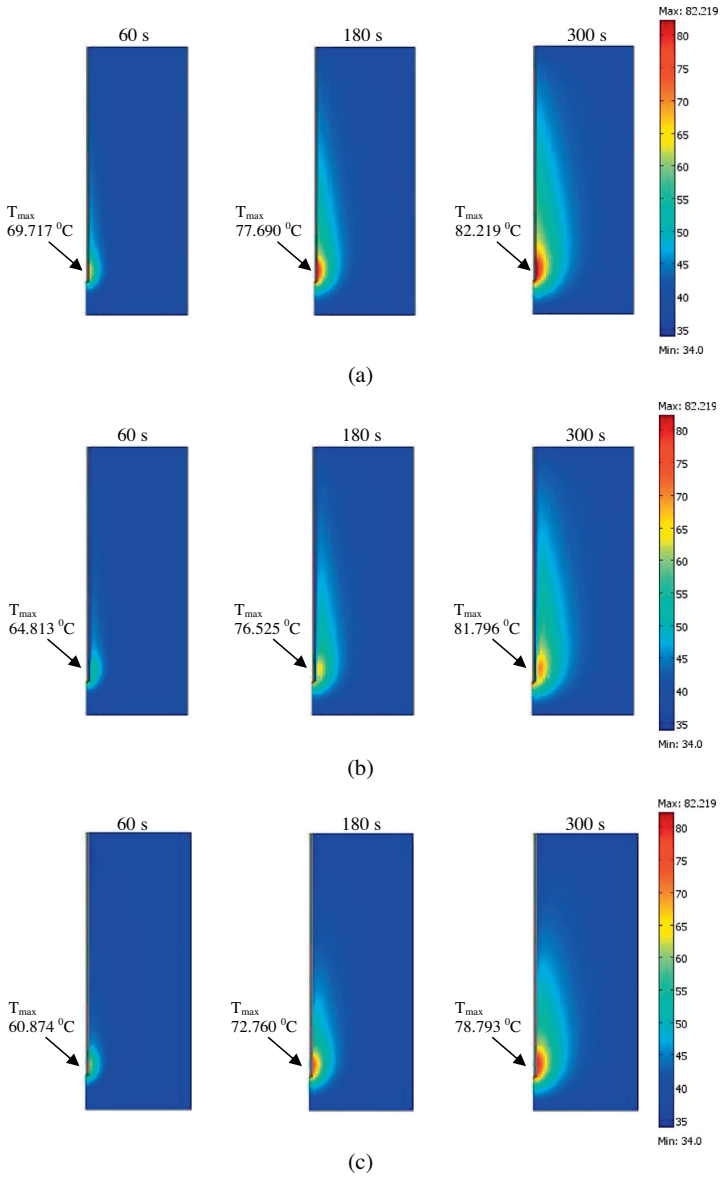

Fig. 9. The temperature profiles in the porous liver at various times where (a) the tissue temperature profiles of LTNE model (b) the blood temperature profiles of LTNE model and (c) the tissue temperature profiles of LTE model based on the same condition in the figure.

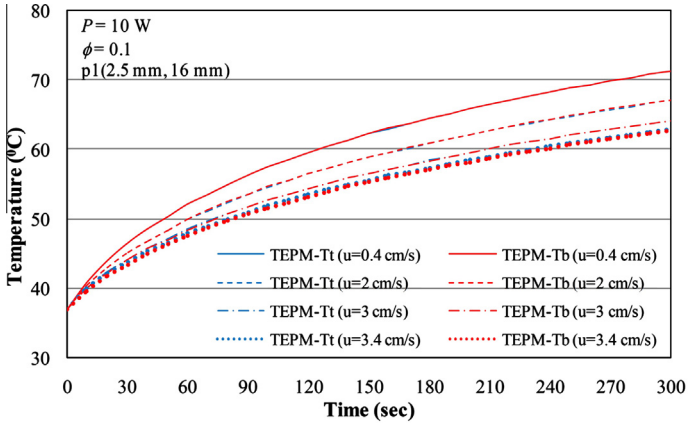

Fig. 10. The tissue and blood temperature distributions of the LTNE model versus time for different blood velocities at the position p1 (r = 2.5 mm, z = 16 mm); (P = 10 W, f = 2.45 GHz, ϕ = 0.1 and t = 300 s).

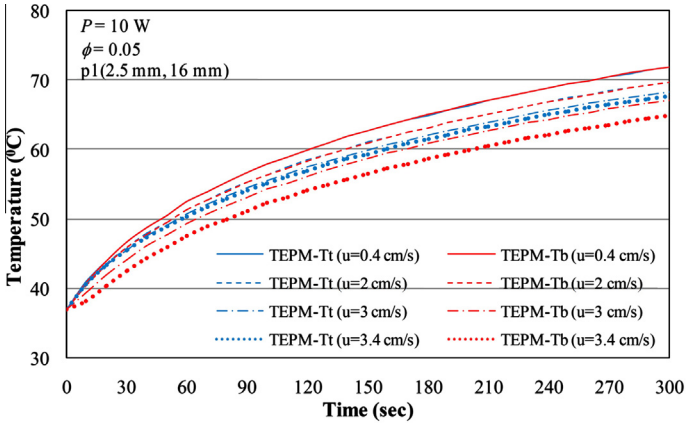

Fig. 11. The tissue and blood temperature distributions of the LTNE model versus time for different blood velocities at the position p1 (r = 2.5 mm, z = 16 mm); (P = 10 W, f = 2.45 GHz, ϕ = 0.05 and t = 300 s).

model within porous liver base on P = 5 W, f = 2.45 GHz, ϕ = 0.025, u = 3.4 cm/s and t = 300 s. From this figure, it is seen that the distribution of tissue and blood temperatures for three positions are increases with an increases in heating time. It is clear that the difference of tissue and blood temperature distributions results at the position of p1 due to position is close to the MCA that hot spot zone occurs. However, the pattern of tissue and blood temperature distributions are similar trends at the position of p2 and p3. Similarly, the temperature at the position of p1has a higher than that of the temperature at the position of p2 and p3, respectively.

In Fig. 15 illustrates the simulated results of tissue and blood temperature distributions of the LTNE model within porous liver at the versus positions when input microwave power is 15 W. The condition is used in this figure based on a same condition as Fig. 14. It is found that the simulation results of Fig. 15 are similar trends to the simulation results in Fig. 14, the distribution of tissue and blood temperatures for three positions are increases with an increases in heating time. Furthermore, the temperature at the position of p1has a higher than that of the temperature at the position of p2 and p3, respectively that are the similar results in Fig. 14. It is clear that the difference of tissue and blood temperatures at the position of p1, a slight difference at the position of p2, whilst, a hardly difference at the position of p3. Greater input microwave power leading to higher difference of temperature for each positions.

The tissue and blood temperature distributions within porous liver at the versus positions when input microwave power is 20 W based on a same condition as Fig. 14 and Fig. 15 is shown in Fig. 16. From the figure, it is seen that the tissue and blood temperature distributions for three positions are increases with an increases in heating time. The temperature at the position of p1has a higher than that of the temperature at the position of p2 and p3, respectively that are the similar results in Fig. 14 and 15. It this figure, the difference of temperature of two phases can be clearly seen at the position of p1 and p2.

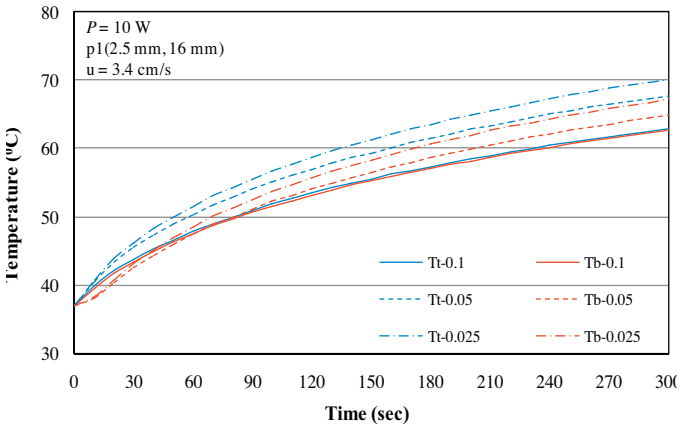

Fig. 13. The tissue and blood temperature distributions of the LTNE model versus time for different porosities at the position p1 (r = 2.5 mm, z = 16 mm); (P = 10 W, f = 2.45 GHz, u = 3.4 cm/s and t = 300 s).

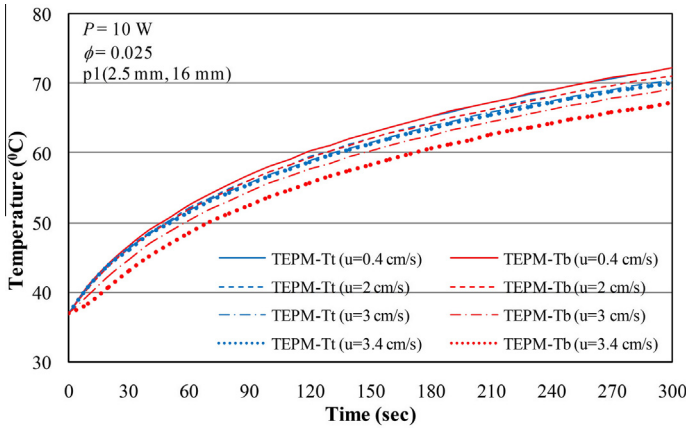

Fig. 12. The tissue and blood temperature distributions of the LTNE model versus time for different blood velocities at the position p1 (r = 2.5 mm, z = 16 mm); (P = 10 W, f = 2.45 GHz, ϕ = 0.025 and t = 300 s).

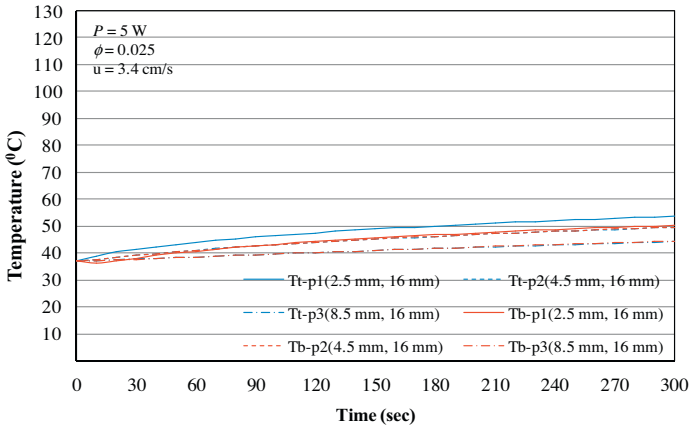

Fig. 14. The tissue and blood temperature distributions of the LTNE model at the versus positions; (P = 5 W, f = 2.45 GHz, ϕ = 0.025, u = 3.4 cm/s and t = 300 s).

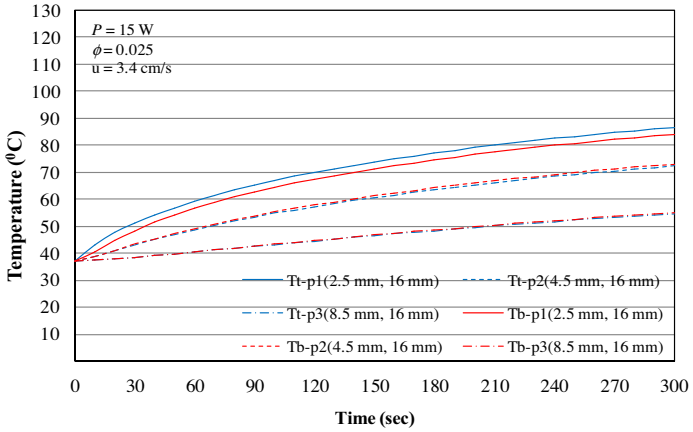

Fig. 15. The tissue and blood temperature distributions of the LTNE model at the versus positions; (P = 15 W, f = 2.45 GHz, ϕ = 0.025, u = 3.4 cm/s and t = 300 s).

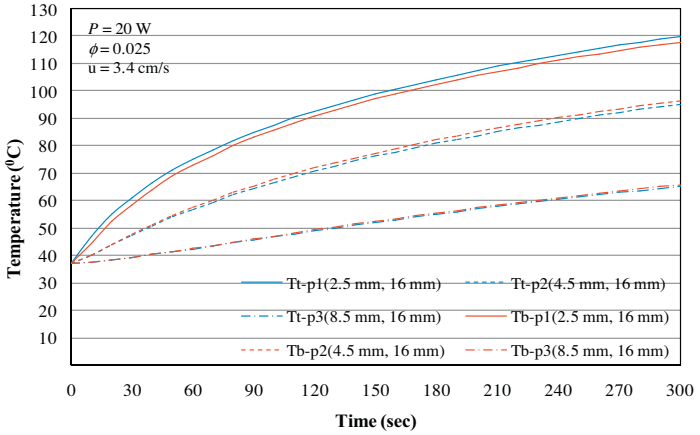

Fig. 16. The tissue and blood temperature distributions of the LTNE model at the versus positions; (P = 20 W, f = 2.45 GHz, ϕ = 0.025, u = 3.4 cm/s and t = 300 s).

Referring to the simulation result in Fig. 14–16, the tissue and blood temperatures in Fig. 16 is higher than that the tissue and blood temperatures in Fig. 14 and Fig. 15 for the same condition and same position. Because of the greater input microwave power leading to higher strength of electric field provides greater heat generation within the porous liver, thereby increasing the tissue and blood temperatures during the MWA process. Furthermore, the greater input microwave power leading to greater difference temperature between the different position. Consider the criterion for use the LTE assumption of the effect of input microwave power, it is difficult to estimate. Because the factors affecting the tissue and blood temperatures include the position. However, it concludes that the input microwave power significantly influence on the tissue and blood temperature distributions within porous liver during MWA process. Nevertheless, in a treatment is often used the heating time for a short time with a higher input microwave power is the trend in thermal therapy [14]. Because of treatment for a longer heating time at low input microwave power will induce a feeling of discomfort and pain for the patient.

Consequently, the above results indicate that the tissue and blood temperatures variation within the porous liver depend on the heating duration, the porosity, the blood velocity, input micro-

wave power and positions within the porous liver during thermal therapy. Although this study analyzes the heat transport within porous media that used only four blood velocities which may not be able to conclude the whole behavior of biological tissue when subjected to electromagnetic fields during thermal ablation. The obtained results can be used as a guideline for the practical treatment.

6. Conclusions

In this study, investigates the transient distribution of tissue and blood temperatures within porous liver during MWA process based on LTNE model undergoing MWA process by MCA. The thermal model considers the tissue with its blood vessel distribution as a porous medium and employs both the convection term due to heat exchange in two phases and blood perfusion term in the transient energy equations for both tissue and blood phases. The tissue and blood temperatures of LTNE model are compared with the tissue temperature of Pennes model and Klinger model. According to the results, the tissue temperature distribution of the Pennes model and the tissue and blood temperature distributions of the LTNE model for blood velocities to be 2 cm/s and 3.4 cm/s when porosity to be 0.05 have similar trends with a difference in magnitude. On the other hand, the temperature distribution pattern of the Klinger model is, very different with the tissue and blood temperatures of LTNE model for all blood velocities. Moreover, the LTE assumption is found to be suitable for predicting the temperature during MWA process when the blood velocities to be 0.4 cm/s and 2 cm/s in all porosities. Conversely, in case blood velocities to be 3 cm/s and 3.4 cm/s the LTNE assumption for heat transfer analysis needs to be utilized. Consistent with the influence of porosity on the different of tissue and blood temperatures, the results show that the lower porosity leading to higher different of tissue and blood temperatures. Therefore, the LTE model is suitable for predicting a distribution of temperature when the high porosity. However, when consider the criterion for use the LTE assumption of the effect of input microwave power, it is difficult to estimate. Because the factors affecting the tissue and blood temperatures include the position. Nevertheless, it concludes that the input microwave power significantly influence on the tissue and blood temperature distributions within porous liver during MWA process.

In next step of this research, will to develop a three-dimensional modeling for approaching realistic liver tissue will be performed. A study will also develop a more realistic model for simulations and study the temperature dependency of and thermal properties of liver tissue.

Acknowledgement

The authors gratefully acknowledge the financial support for this work provided by the Thailand Research Fund (TRF).

References

[1] T. Peng, D.P. O'Neill, S.J. Payne, A two-equation coupled system for determination of liver tissue temperature during thermal ablation, Int. J. Heat Mass Transf. 54 (9–10) (2011) 2100–2109.
[2] C.J. Simon, D.E. Dupuy, W.W. Mayo-Smith, Microwave ablation: principles and applications, Radiographics 25 (Special Issue) (2005) S69–S83.
[3] J.P. McGahan, J.M. Brock, H. Tesluk, W.Z. Gu, P. Schneider, P.D. Browing, Hepatic ablation with use of radio-frequency electrocautery in the animal model, J. Vasc. Intervent. Radiol.: JVIR 3 (2) (1992) 291–297.
[4] H.H. Pennes, Analysis of tissue and arterial blood temperatures in the resting human forearm, J. Appl. Physiol. 85 (1) (1998) 5–34.
[5] J. Okajima, S. Maruyama, H. Takeda, A. Komiya, Dimensionless solutions and general characteristics of bioheat transfer during thermal therapy, J. Therm. Biol 34 (8) (2009) 377–384.
[6] P. Phasukkit, S. Tungjitkusolmun, M. Sangworasil, Finite-element analysis and in vitro experiments of placement configurations using triple antennas in microwave hepatic ablation, IEEE Trans. Biomed. Eng. 56 (11) (2009) 2564–2572.
[7] M. Liangruksa, R. Ganguly, I.K. Puri, Parametric investigation of heating due to magnetic fluid hyperthermia in a tumor with blood perfusion, J. Magn. Magn. Mater. 323 (6) (2011) 708–716.
[8] S. Becker, Analytic one dimensional transient conduction into a living perfuse/non-perfuse two layer composite system, Heat Mass Transf. 48 (2) (2012) 317–327.
[9] H. Klinger, Heat transfer in perfused biological tissue I: general theory, Bull. Math. Biol. 36 (4) (1974) 403–415.
[10] D. Yang, M. Converse, D. Mahvi, Expanding the bioheat equation to include tissue internal water evaporation during heating, IEEE Trans. Biomed. Eng. 54 (8) (2007) 1382–1388.
[11] P. Keangin, T. Wessapan, P. Rattanadecho, Analysis of heat transfer in deformed liver cancer modeling treated using a microwave coaxial antenna, Appl. Therm. Eng. 31 (16) (2011) 3243–3254.
[12] W. Roetzel, Y. Xuan, Transient response of the human limb to an external stimulust, Int. J. Heat Mass Transf. 41 (1) (1998) 229–239.
[13] A. Nakayama, F. Kuwahara, A general bioheat transfer model based on the theory of porous media, Int. J. Heat Mass Transf. 51 (2008) 3190–3199.
[14] P. Yuan, Numerical analysis of temperature and thermal dose response of biological tissues to thermal non-equilibrium during hyperthermia therapy, Med. Eng. Phys. 30 (2) (2008) 135–143.
[15] B. Alazmi, K. Vafai, Analysis of variants within the porous media transport models, ASME J. Heat Transfer 122 (2000) 303–326.
[16] A.-R.A. Khaled, K. Vafai, The role of porous media in modeling flow and heat transfer in biological tissues, Int. J. Heat Mass Transf. 46 (2003) 4989–5003.
[17] H.S. Kou, T.C. Shih, W.L. Lin, Effect of the directional blood flow on thermal dose distribution during thermal therapy: an application of a Green's function based on the porous model, Phys. Med. Biol. 48 (11) (2003) 1577–1589.
[18] P. Rattanadecho, P. Keangin, Numerical study of heat transfer and blood flow in two-layered porous liver tissue during microwave ablation process using single and double slot antenna, Int. J. Heat Mass Transf. 58 (1–2) (2013) 457–470.
[19] W. Klinbun, K. Vafai, P. Rattanadecho, Electromagnetic field effects on transport through porous media, Int. J. Heat Mass Transf. 55 (1–3) (2012) 325–335.
[20] J. Fan, L. Wang, A general bioheat model at macroscale, Int. J. Heat Mass Transf. 54 (1–3) (2011) 722–726.
[21] N. Afrin, Y. Zhang, J.K. Chen, Thermal lagging in living biological tissue based on nonequilibrium heat transfer between tissue, arterial and venous bloods, Int. J. Heat Mass Transf. 54 (11–12) (2011) 2419–2426.
[22] S. Mahjoob, K. Vafai, Analytical characterization of heat transport through biological media incorporating hyperthermia treatment, Int. J. Heat Mass Transf. 52 (5–6) (2009) 1608–1618.
[23] P. Yuan, Numerical analysis of an equivalent heat transfer coefficient in a porous model for simulating a biological tissue in a hyperthermia therapy, Int. J. Heat Mass Transf. 52 (7–8) (2009) 1734–1740.
[24] A. Belmiloudi, Parameter identification problems and analysis of the impact of porous media in biofluid heat transfer in biological tissues during thermal therapy, Nonlinear Anal.: Real World Appl. 11 (3) (2010) 1345–1363.
[25] K. Saito, Y. Hayashi, H. Yoshimura, K. Ito, Heating characteristics of array applicator composed of two coaxial-slot antennas for microwave coagulation therapy, IEEE Trans. Microw. Theory Tech. 48 (2000) 1800–1806 (1 PART 1).
[26] C.W. Song, Role of blood flow in hyperthermia, in: M. Urano, E. Douple (Eds.), Hyperthermia and Oncology Interstitial Hyperthermia: Physics, Biology and Clinical Aspects, Utrecht, VSP, 1992, pp. 275–315.
[27] Y. Zhang, Generalized dual-phase lag bioheat equations based on nonequilibrium heat transfer in living biological tissues, Int. J. Heat Mass Transf. 52 (21–22) (2009) 4829–4834.
[28] T. Wessapan, S. Srisawatdhisukul, P. Rattanadecho, The effects of dielectric shield on specific absorption rate and heat transfer in the human body exposed to leakage microwave energy, Int. Commun. Heat Mass Transfer 38 (2) (2011) 255–262.
[29] J. Crezee, J.J.W. Lagendijk, Temperature uniformity during hyperthermia: the impact of large vessels, Phys. Med. Biol. 37 (6) (1992) 1321–1337.
[30] J.M. Bertram, D. Yang, M.C. Converse, Antenna design for microwave hepatic ablation using an axisymmetric electromagnetic model, Biomed. Eng. Online 5 (2006).
[31] P. Keangin, P. Rattanadecho, T. Wessapan, An analysis of heat transfer in liver tissue during microwave ablation using single and double slot antenna, Int. Commun. Heat Mass Transfer 38 (6) (2011) 757–766.
[32] J.M. Bertram, M.C. Converse, A.P. O'Rourke, J.G. Webster, S.C. Hagness, J.A. Will, D.M. Mahvi, A floating sleeve antenna yields localized hepatic microwave ablation, IEEE Trans. Biomed. Eng. 53 (3) (2006) 533–537.
[33] M.S. Malashetty, M. Swamy, R. Heera, Double diffusive convection in a porous layer using a thermal non-equilibrium model, Int. J. Therm. Sci. 47 (9) (2008) 1131–1147.
[34] A. Vera, L. Leija, Microcoaxial Double slot antenna for interstitial hyperthermia: design, modeling and validation, in: International Conference on Advances in Electronics and Micro-electronics ENICS'08, 2008, pp. 138–143.
[35] Y. Rabin, A. Shitzer, Numerical solution of the multidimensional freezing problem during cryosurgery, J. Biomech. Eng. 120 (1) (1998) 32–37.
[36] J. Lienhard, A Heat Transfer Textbook, Lexington, Phlogiston, MA, 2005.
[37] C. Thiebaut, D. Lemonnier, Three-dimensional modelling and optimisation of thermal fields induced in a human body during hyperthermia, Int. J. Therm. Sci. 41 (6) (2002) 500–508.
[38] F.A. Duck, A.C. Baker, H.C. Starrit, Ultrasound in Medicine, Institute of Physics Publishing, London, 1998. 57-88.